How to cite: *Angew. Chem. Int. Ed.* **2020**, *59*, 20230–20234
International Edition: doi.org/10.1002/anie.202008646
German Edition: doi.org/10.1002/ange.202008646

Black Phosphorus

Quantifying the Covalent Functionalization of Black Phosphorus

Stefan Wild, Xuan Thong Dinh, Harald Maid, Frank Hauke, Gonzalo Abellán, and Andreas Hirsch**

Abstract: *A straightforward quantification method to consistently determine the overall functionalization degree of covalently modified two-dimensional (2D) black phosphorus (BP) by Raman spectroscopy has been carried out. Indeed, the successful reductive methylation of the BP lattice using sodium intercalation compounds and exhibiting different functionalization degrees has been demonstrated by ^{31}P-magic angle spinning (MAS) NMR spectroscopy. Furthermore, the correlation of ^{31}P-MAS NMR spectroscopy and statistical Raman spectroscopy (SRS) revealed the first method to determine the functionalization degree of BP solely by evaluating the intensities of distinct peaks in the Raman spectra of the covalently modified material, in a similar way to the widely employed I_D/I_G ratio of graphene research.*

Among the quickly expanding family of two dimensional (2D) materials black phosphorous (BP) has attracted enormous attention in the last years due to its high p-type charge carrier mobility and its tunable direct band gap.[1] BP possesses a puckered honeycomb crystal lattice, in which P atoms are covalently bound to three adjacent neighbors with one remaining free electron pair on each P atom. In contrast to its intensively studied intrinsic materials properties, the chemical modification of BP is still in its infancy.[2] In fact, the non-covalent functionalization of its 2D surface with perylene bisimide derivatives was pioneered in order to protect BP from degradation under ambient conditions.[3] Later on, special attention was paid towards the covalent modification of BP, as this is probably the most promising alternative for the precise tuning of both the chemical and physical properties of 2D nanomaterials.[4] Along this route, the working group of Hersam described the covalent modification of the BP surface by the immersion of micromechanically exfoliated BP flakes in a solution of diazonium salts.[5] This work was followed by several wet chemical approaches to process previously exfoliated BP by the use of nucleophilic reagents,[6] iodonium salts[7] or carbon free radicals.[8] However, very low functionalization degrees, and the absences of clear spectroscopic fingerprints of the successful covalent functionalization were common issues. Moreover, an explicit determination of the underlying mechanisms as well as the terminal binding motif of the covalently modified BP remained as open questions. For this reasons, we adapted the already well-known reductive covalent functionalization strategy in graphene chemistry, which makes use of graphite intercalation compounds (GICs).[4a,9] In a first step we therefore reported the production of BP intercalation compounds (BPICs) via solid state insertion of alkali metals (AMs).[10] This novel compound class also enables the distinct preparation of BP nanoribbons when exfoliated in *N*-methyl pyrrolidone (NMP).[11] Following the reductive route we decided to implement the use of BPICs in our reaction sequence. Upon the addition of an electrophilic alkyl halide after dispersing the BPIC in an inert solvent like tetrahydrofurane (THF), a drastic increase of the functionalization degree took place. Furthermore, we were able to demonstrate that P–P bond breakage occurs during the covalent attachment of the electrophile, which was unambiguously proven by ^{31}P magic angle spinning (MAS) solid state NMR spectroscopy.[12] However, a straightforward, unequivocal and consistent determination of the functionalization degree of 2D BP remains an open challenge of utmost importance.

Herein, the covalent functionalization of BP starting from BPICs having different amounts of sodium was achieved by the addition of iodomethane (MeI). This reaction yields covalently modified BP with varying functionalization degrees. ^{31}P-MAS solid state NMR spectroscopy unambiguously proved the successful methylation of BP.

In addition, statistical Raman spectroscopy (SRS) studies exhibit novel characteristic modes in the high-energy region, which can be energetically assigned to the P–C and C–H vibration, respectively both originating from the covalently attached methyl group on the BP surface. Correlating these vibrational Raman modes to the directly determined functionalization degree by ^{31}P-MAS solid state NMR spectroscopy allows the convenient determination of the overall functionalization degree only by non-time consuming Raman Spectroscopy, paving the way for the development of the covalent chemistry in 2D BP.

[*] S. Wild, X. T. Dinh, Dr. H. Maid, Dr. F. Hauke, Dr. G. Abellán, Prof. A. Hirsch
Chair of Organic Chemistry II and Joint Institute of Advanced Materials and Processes (ZMP); Friedrich-Alexander-Universität Erlangen-Nürnberg (FAU)
Nikolaus-Fiebiger Straße 10, 91058 Erlangen and Dr.-Mack Straße 81, 90762 Fürth (Germany)
E-mail: gonzalo.abellan@fau.de
andreas.hirsch@fau.de
Dr. G. Abellán
Instituto de Ciencia Molecular (ICMol), Universidad de Valencia
Catedrático José Beltrán 2, 46980, Paterna, Valencia (Spain)
E-mail: gonzalo.abellan@uv.es
Supporting information and the ORCID identification number(s) for the author(s) of this article can be found under https://doi.org/10.1002/anie.202008646.

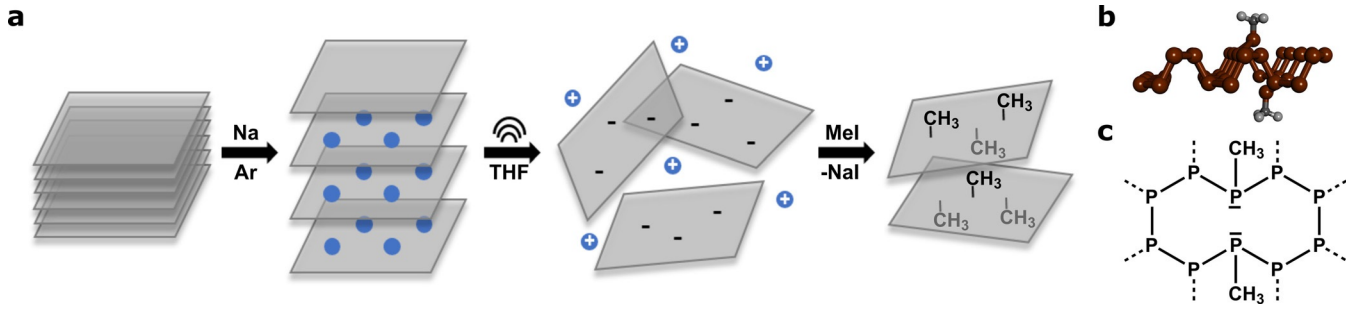

Scheme 1. (a) Reaction sequence displaying the reductive covalent methylation of BP. (b) Side view of a covalently functionalized BP layer bearing two methyl groups. (c) Chemical structure of methylated BP showcasing the lattice opening of BP upon its covalent modification.

Scheme 1a displays the general reaction sequence that was applied in order to attach the methyl group covalently onto the 2D BP surface. First, bulk BP was intercalated via our previously described solid state method using different amounts of sodium to yield the respective BPICs NaP_x.[10] We selected sodium due to its milder character and higher stability compared to potassium BPICs, which may be related to the formation of cation-π passivation layers.[12a,13] Afterwards, the BPICs were dispersed in purified THF utilizing ultra-sonication which produces negatively charged exfoliated BP sheets. To trap these negative charges, the electrophile MeI was added to the BP dispersion. Consequently, the methylation of the BP takes place in a nucleophilic substitution reaction, while NaI is formed as a byproduct. Lastly, the dispersion is filtered and the obtained covalently functionalized BP powder was washed multiple times with THF.

Again, it is important to mention that upon this reductive covalent modification a lattice opening of BP takes place, which originates from an in-plane P–P bond breakage, this fact will probably impose electrostatic and steric limitations in the functionalization degree. As a side effect the methylated P-atom gets slightly pulled out of the 2D plane.[12a] The resulting schematic structure of the methylated BP lattice is illustrated in Scheme 1b,c. The typical Raman spectrum of methylated BP—exemplified for the reaction of the BPIC NaP_4 with MeI—can be seen in Figure 1a. Besides the three characteristic Raman modes of BP at 361, 435 and 466 cm^{-1} several additional peaks can be observed. To begin, the typical Raman feature for covalently modified BP is detected in the low wavenumber region below 300 cm^{-1}, which was identified in our last report to originate from BP lattice distortions caused by the attached addend.[12a] Remarkably, at 645 and 773 cm^{-1} (Figure 1b) two more prominent peaks appear (marked in blue), which energetically fit to the covalent P–C bond and therefore are labelled as "P–C".[14] It is worth mentioning that the direct visualization of the covalent P–C bond on BP by Raman spectroscopy has not been reported so far. Moreover, we detected two additional major Raman modes at 2900 and 2970 cm^{-1} (marked in orange), which perfectly fit to the "C–H" stretching modes of the methyl group. The minor peaks between 1280 and 1430 cm^{-1} can be assigned to the asymmetric stretching of the P–CH_3 unit. Comparing the mean Raman spectrum of methylated BP to pure MeI shows no agreement confirming that all the discussed Raman modes definitely originate from the covalent modification of BP (SI 1)

Next, we hypothesize that this direct observation of the covalent P–C bond could enable the quantification of the functionalization degree only by Raman Spectroscopy. Thus, the idea is to correlate the measured intensity of the P–C vibrational contribution for the different samples to the most prominent BP Raman mode, which is the A^2_g mode at 466 cm^{-1}. In order to produce samples with varying functionalization degrees we decided to use BPICs with different amounts of the AM—namely NaP_4, NaP_6 and NaP_{12}—in our reaction sequence. The more activated the BP is due to the charge transfer from the AM to its 2D lattice, the more functionalization should occur. However, we did not exceed

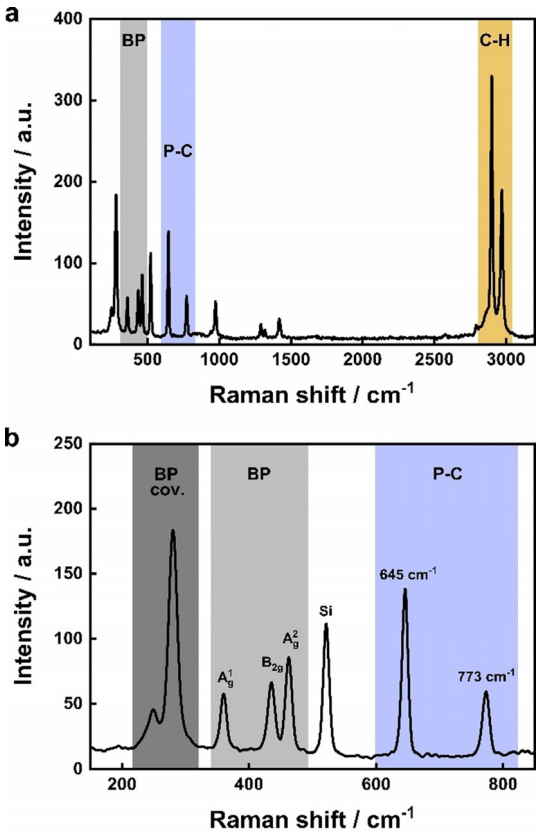

Figure 1. a) Mean Raman spectrum of methylated NaP_4 and the related zoom in (b) highlighting the low wavenumber region.

the limit of 0.25 mol of the AM per phosphorus atom because that would result in the irreversible formation of intermetallic alloys.[10,15] Among these undesired alloys, Na_3P is the thermodynamically most stable one, but there are also several other Zintl phase-like compounds whose formation causes the complete destruction of the BP lattice.[16] First of all we conducted XPS measurements confirming the formation of P–C bonds and showing a remarkably low oxidized phosphorus $P^{P\text{-}O}$ contributions. Moreover, a clear trend (showing higher intensity for the higher amounts of sodium) can be observed when analyzing the chemical shift of +2.7 eV relative to the P^0 signal, indicative of carbon-bound species (see SI 2).

In Figure 2a the intensity ratio of the C–H vibrational mode versus the A^2_g band of BP for the three respective BPICs is displayed. It is obvious that with increasing amount of the AM the C–H/A^2_g ratio is also rising. The same trend can be observed when comparing the intensity of the P–C vibrational mode at 645 cm^{-1} versus the A^2_g peak of BP (Figure 2b). Both plots originate from a statistical evaluation of the associated Raman mappings on functionalized BP for each of the different BPICs. Additionally, the mean spectra of the three Raman mappings (minimum 15×15 μm, step 0.5 μm) can be seen in SI 3. In case of the C–H/A^2_g ratio, the extracted mean value increases from around 0.52±0.11 in NaP_{12} up to 3.48±0.46 in NaP_4. Simultaneously, the P–C/A^2_g ratio varies between 0.24±0.06 in NaP_{12} up to 1.57±0.26 in NaP_4. Also, Raman maps show that the functionalization

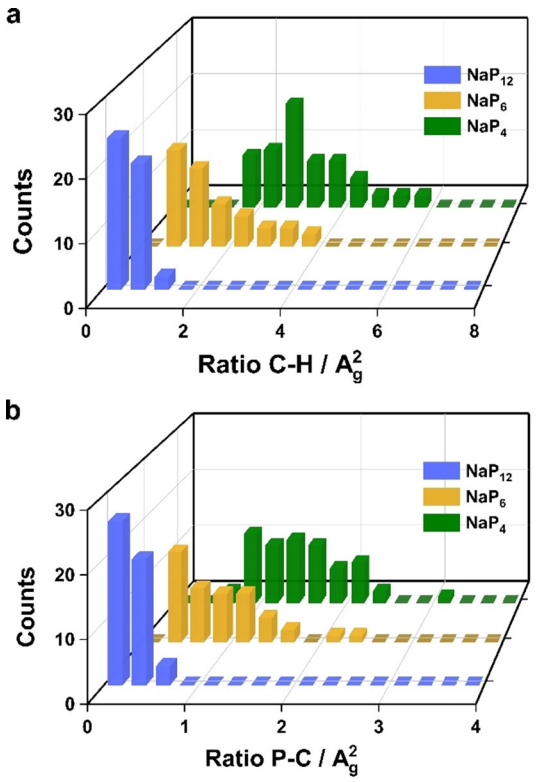

Figure 2. 3D plot showing the statistical evaluation of the Raman mappings featuring the C–H/A^2_g ratio (a) and the P–C/A^2_g ratio (b) for the respective BPICs NaP_4, NaP_6 and NaP_{12}.

arises homogeneously on BP flakes (SI 4&5). These results offer the possibility to correlate the functionalization degree of methylated BP to an intensity ratio of distinct Raman modes, similar to the I_D/I_G ratio in graphene chemistry.[17]

Along this route, we measured quantitative ^{31}P-MAS solid state NMR spectroscopy (using a Bruker NEO 500 MHz spectrometer) of the methylated BP samples, which were previously characterized by SRS. This will allow to exactly determine the functionalization degree of the covalently modified reaction products, thus enabling the desired correlation to the measured Raman intensity ratios. A typical ^{31}P-MAS NMR spectrum of methylated BP can be seen in Figure 3a. The main peak at a chemical shift of 18.2 ppm can be assigned to pristine BP, whereas the small shoulder at 23.7 ppm is caused by the covalent attachment of the methyl group as well as the accompanied breakage of one P–P bond in the BP lattice yielding a phosphine like $P_2P\text{-}CH_3$-species.[12a] Figure 3b compares the recorded NMR spectra of the reaction products when using varying amounts of intercalated AM. Again, the shoulder representing the covalent modification of the BP lattice at 23.7 ppm gets more pronounced with increasing amounts of sodium. This trend is in excellent agreement with the prior discussed Raman results. In fact, by applying a deconvolution to each of the spectra, the exact functionalization degree could be determined to be 1.9% for NaP_{12}, 2.8% for NaP_6 and 4.7% for NaP_4 respectively. Furthermore, ^{13}C-MAS solid state NMR spectroscopy confirmed the presence of methyl groups in all the covalently modified reaction products (SI 6). These values can be considered as a high degree of functionalization and are slightly smaller to that previously described by our group for potassium KP_6 BPICs (ca. 7%).[12a] In this sense, it should be mentioned that intervals between fabrication and subsequent NMR characterization were kept constant at 48 h, to ensure comparability between samples. Moreover, the dynamic behavior exhibited by the BPICS may induce some variations in the activation of BP, and therefore in the final functionalization degree. In any case, using sodium instead of potassium has no significant influence on the overall functionalization degree (SI 7).

Last but not least, correlating these ^{31}P-MAS NMR results to the C–H/A^2_g and P–C/A^2_g Raman ratios yields a clear trend (Figure 3c) indicating that SRS indeed is a suitable technique to quickly estimate the functionalization degree of methylated BP. It is worth to mention that a calibration curve is always required, as different Raman spectrometers/measurement conditions (e.g. changing the excitation wavelength) may induce slight variations in the intensity ratios (see SI 8&9).

To conclude, we have established the first systematic quantification method to determine the overall functionalization degree of methylated BP by non-time consuming statistical Raman Spectroscopy. Therefore, we correlated novel Raman modes—specifically at 645 cm^{-1} and 2900 cm^{-1}—which originate from the covalent modification of the BP lattice to the quantitatively determined functionalization degree obtained by ^{31}P-MAS solid state NMR Spectroscopy. Since Raman spectroscopy is one of the most powerful characterization tools in materials chemistry, as

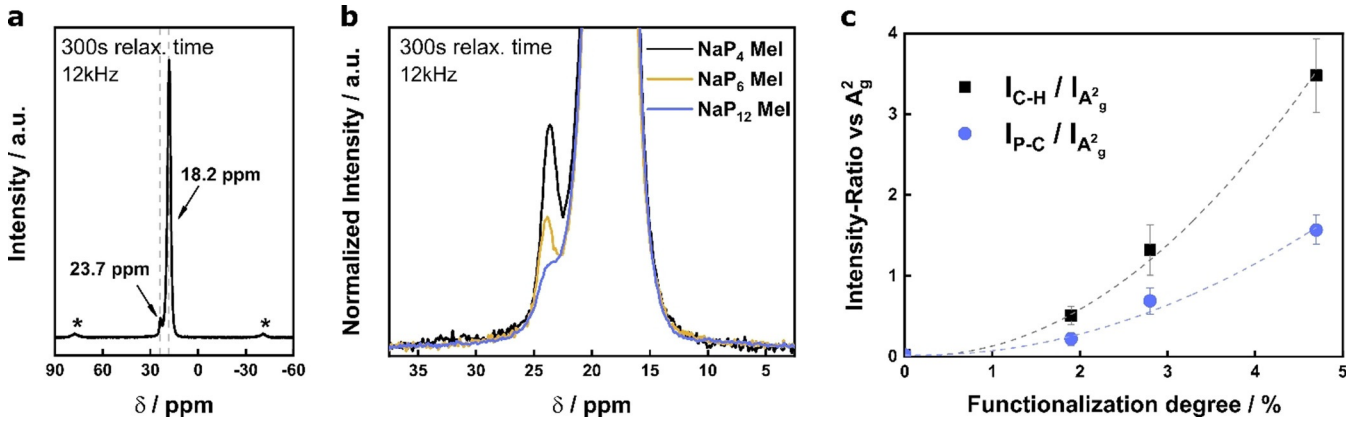

Figure 3. (a) Full range ^{31}P-MAS solid state NMR spectrum of methylated BP—exemplary for the reaction product of NaP_4 with MeI. (b) Zoom in highlighting the comparison of ^{31}P-MAS solid state NMR spectra of methylated BP starting from different BPICs. (c) Correlation of the functionalization degree determined by quantitative ^{31}P-MAS solid state NMR spectroscopy to the Raman intensity ratio of the C—H and P—C vibrational mode versus the A^2_g mode of BP.

evidenced by graphene research, these results will foster the progression in the field of 2D BP research. Especially for the quick evaluation of alternative functionalization protocols the presented correlation method could be of great use to determine the efficiency of the chosen reaction pathway.

Experimental Section

BP crystals were purchased from Smart Elements (< 99,999 % purity) and mortared before elemental sodium was mixed with the BP powder in the respective stoichiometry in order to yield the different BPICs. The intercalation was performed according to our previously described solid state preparation method.[10] THF (anhydrous) was bought from Sigma Aldrich and degassed by the Pump-Freeze-Thaw method before it was introduced in an Argon filled glove box (< 0.1 ppm O_2 and H_2O). For the covalent functionalization process the respective BPIC (0.5 mmol) was first dispersed in purified THF, and subsequently ultra-sonication (25 %, 5 min, 2 s pulse) using a Bandelin SONOPULS HD4100 sonotrode was applied to yield negatively charged BP sheets. Afterwards iodomethane (0.5 mmol) was added and the dispersion was stirred for 24 h. Filtration and subsequent washing of the samples with THF inside the glove box yielded the reaction products as grey powder. Raman characterization of all products was carried out using a WiTec alpha300 R confocal microscope equipped with an XYZ table. Statistical evaluation of individual maxima for each Raman mode was accomplished by applying a filter in the desired energy region. Subsequent division of absolute intensities yielded the statistical distribution of the respective intensity ratios P-C/A^2_g and C-H/A^2_g. The mean values of these statistical distributions were extracted by using a standard gaussian fit within each histogram. Throughout all measurements, an excitation wavelength of 532 nm, an acquisition time of 0.5 s and a laser power of 5 mW was used. The step size was chosen to be 0.5 μm throughout all Raman mappings, whose sizes were varying from 15 × 15 μm up to 30 × 30 μm. For comparison, Raman spectra of all methylated BP samples were acquired also with a LabRam HR Evolution confocal Raman microscope (Horiba) equipped with an automated XYZ table using 0.80 NA objectives. ^{31}P-MAS solid state NMR spectra were recorded on a Bruker NEO 500 MHz spectrometer operating at the ^{13}C and ^{31}P frequencies of 125.81 and 202.54 MHz, respectively. All the samples were spun at 12 kHz in a double resonance MAS probe (PH MAS VTN 500S1 BL4 N-P/H) designed for 4 mm o.d. rotors. Due to the limited amount of sample, zirconia rotors with a reduced sample volume of 12 μL were used. To avoid oxidation, the reaction products were filled already inside the glovebox into the rotor (NaP_4: 11 mg; NaP_6: 13 mg; NaP_{12}: 15 mg). For the ^{31}P measurements the one-pulse sequence was used with a recycle delay of 300 s to ensure complete relaxation of all nuclei. The spectral width was set to 100 kHz and 16 transients for NaP_4 and 32 transients for NaP_6 and NaP_{12} per FID were acquired on 5000 time domain points. No filter function was applied and the FID was zero filled to 8192 data points prior to Fourier transform. For the ^{13}C CPMAS experiments a recycle delay of 5 s, 1H-13C Hartman-Hahn contact period of 2 ms with a 50 % to 100 % ramp (ramp50100.100) and an initial 1H π/2-pulse width of 2.3 μs were common to all CPMAS data. Proton decoupling during acquisition was done using the SPINAL-64 decoupling Scheme. The spectral width was set to 38.5 kHz and 40000 transients for NaP_{12} and 12000 transients for NaP_6 and NaP_4 per FID were acquired on 2k time domain points. A line broadening of 30 Hz was applied and the FID was zero filled to 8192 data points prior to Fourier transform. Chemical shifts were calibrated using adamantane as a secondary reference.

Acknowledgements

A.H. and G.A. acknowledge the European Research Council (ERC Advanced Grant 742145 B-PhosphoChem to A.H., and ERC Starting Grant 2D-PnictoChem 804110 to G.A.) for support. The research leading to these results was partially funded by the European Union Seventh Framework Programme under grant agreement No. 604391 Graphene Flagship. A.H. thank the Sonderforschungsbereich (SFB) 953 "Synthetic Carbon Allotropes" funded by the Deutsche Forschungsgemeinschaft (DFG) for support, and the Cluster of Excellence "Engineering of Advanced Materials". G.A. acknowledges support by the Generalitat Valenciana (CIDEGENT/2018/001 and iDiFEDER/2018/061 co-financed by FEDER), the Spanish MICINN (PID2019-111742GA-I00 and Excellence Unit María de Maeztu (CEX2019-000919-M)), and the DFG (FLAG-ERA AB694/2-1). Special thanks to Antonio Leyva-Pérez and José Alejandro Vidal-Moya from ITQ Valencia for their kind assistance in ^{31}P MAS NMR data processing. Open access funding enabled and organized by Projekt DEAL.

Conflict of interest

The authors declare no conflict of interest.

Keywords: ^{31}P-MAS NMR spectroscopy · black phosphorus · covalent functionalization · Raman spectroscopy · reduction

[1] a) A. Castellanos-Gomez, L. Vicarelli, E. Prada, J. O. Island, K. L. Narasimha-Acharya, S. I. Blanter, D. J. Groenendijk, M. Buscema, G. A. Steele, J. V. Alvarez, H. W. Zandbergen, J. J. Palacios, H. S. J. van der Zant, *2D Mater.* **2014**, *1*, 025001; b) L. Li, Y. Yu, G. J. Ye, Q. Ge, X. Ou, H. Wu, D. Feng, X. H. Chen, Y. Zhang, *Nat. Nano* **2014**, *9*, 372 – 377; c) H. Liu, A. T. Neal, Z. Zhu, Z. Luo, X. Xu, D. Tománek, P. D. Ye, *ACS Nano* **2014**, *8*, 4033 – 4041; d) J. D. Wood, S. A. Wells, D. Jariwala, K.-S. Chen, E. Cho, V. K. Sangwan, X. Liu, L. J. Lauhon, T. J. Marks, M. C. Hersam, *Nano Lett.* **2014**, *14*, 6964 – 6970; e) S. P. Koenig, R. A. Doganov, H. Schmidt, A. H. Castro Neto, B. Özyilmaz, *Appl. Phys. Lett.* **2014**, *104*, 103106; f) A. Castellanos-Gomez, *J. Phys. Chem. Lett.* **2015**, *6*, 4280 – 4291; g) F. Xia, H. Wang, Y. Jia, *Nat. Commun.* **2014**, *5*, 4458; h) J. Qiao, X. Kong, Z.-X. Hu, F. Yang, W. Ji, *Nat. Commun.* **2014**, *5*, 4475; i) Z. Sofer, D. Sedmidubský, Š. Huber, J. Luxa, D. Bouša, C. Boothroyd, M. Pumera, *Angew. Chem. Int. Ed.* **2016**, *55*, 3382 – 3386; *Angew. Chem.* **2016**, *128*, 3443 – 3447.

[2] a) A. Hirsch, F. Hauke, *Angew. Chem. Int. Ed.* **2018**, *57*, 4338 – 4354; *Angew. Chem.* **2018**, *130*, 4421 – 4437; b) R. Gusmão, Z. Sofer, M. Pumera, *Angew. Chem. Int. Ed.* **2017**, *56*, 8052 – 8072; *Angew. Chem.* **2017**, *129*, 8164 – 8185.

[3] a) G. Abellán, V. Lloret, U. Mundloch, M. Marcia, C. Neiss, A. Görling, M. Varela, F. Hauke, A. Hirsch, *Angew. Chem. Int. Ed.* **2016**, *55*, 14557 – 14562; *Angew. Chem.* **2016**, *128*, 14777 – 14782; b) O. J. O. Island, G. A. Steele, H. S. J. van der Zant, A. Castellanos-Gomez, *2D Mater.* **2015**, *2*, 011002; c) G. Abellán, S. Wild, V. Lloret, N. Scheuschner, R. Gillen, U. Mundloch, J. Maultzsch, M. Varela, F. Hauke, A. Hirsch, *J. Am. Chem. Soc.* **2017**, *139*, 10432 – 10440; d) Y. Zhao, Q. Zhou, Q. Li, X. Yao, J. Wang, *Adv. Mater.* **2016**, 1603990; e) W. Sumeet, S. Ylias, A. Taimur, R. F. Matthew, R. Rajesh, A. Aram, K. B. Suresh, S. Sharath, B. Madhu, B. Vipul, B. Sivacarendran, *2D Mater.* **2017**, *4*, 015025.

[4] a) J. M. Englert, C. Dotzer, G. Yang, M. Schmid, C. Papp, J. M. Gottfried, H.-P. Steinrück, E. Spiecker, F. Hauke, A. Hirsch, *Nat. Chem.* **2011**, *3*, 279; b) D. Voiry, A. Goswami, R. Kappera, C. d. C. C. e. Silva, D. Kaplan, T. Fujita, M. Chen, T. Asefa, M. Chhowalla, *Nat. Chem.* **2015**, *7*, 45.

[5] C. R. Ryder, J. D. Wood, S. A. Wells, Y. Yang, D. Jariwala, T. J. Marks, G. C. Schatz, M. C. Hersam, *Nat. Chem.* **2016**, *8*, 597 – 602.

[6] Z. Sofer, J. Luxa, D. Bouša, D. Sedmidubský, P. Lazar, T. Hartman, H. Hardtdegen, M. Pumera, *Angew. Chem. Int. Ed.* **2017**, *56*, 9891 – 9896; *Angew. Chem.* **2017**, *129*, 10023 – 10028.

[7] M. van Druenen, F. Davitt, T. Collins, C. Glynn, C. O'Dwyer, J. D. Holmes, G. Collins, *Chem. Mater.* **2018**, *30*, 4667 – 4674.

[8] H. Hu, H. Gao, L. Gao, F. Li, N. Xu, X. Long, Y. Hu, J. Jin, J. Ma, *Nanoscale* **2018**, *10*, 5834 – 5839.

[9] P. Vecera, J. Holzwarth, K. F. Edelthalhammer, U. Mundloch, H. Peterlik, F. Hauke, A. Hirsch, *Nat. Commun.* **2016**, *7*, 12411.

[10] G. Abellán, C. Neiss, V. Lloret, S. Wild, J. C. Chacón-Torres, K. Werbach, F. Fedi, H. Shiozawa, A. Görling, H. Peterlik, T. Pichler, F. Hauke, A. Hirsch, *Angew. Chem. Int. Ed.* **2017**, *56*, 15267 – 15273; *Angew. Chem.* **2017**, *129*, 15469 – 15475.

[11] M. C. Watts, L. Picco, F. S. Russell-Pavier, P. L. Cullen, T. S. Miller, S. P. Bartuś, O. D. Payton, N. T. Skipper, V. Tileli, C. A. Howard, *Nature* **2019**, *568*, 216 – 220.

[12] a) S. Wild, M. Fickert, A. Mitrovic, V. Lloret, C. Neiss, J. A. Vidal-Moya, M. Á. Rivero-Crespo, A. Leyva-Pérez, K. Werbach, H. Peterlik, M. Grabau, H. Wittkämper, C. Papp, H.-P. Steinrück, T. Pichler, A. Görling, F. Hauke, G. Abellán, A. Hirsch, *Angew. Chem. Int. Ed.* **2019**, *58*, 5763 – 5768; *Angew. Chem.* **2019**, *131*, 5820 – 5826; b) L. Zhang, L.-F. Gao, L. Li, C.-X. Hu, Q.-Q. Yang, Z.-Y. Zhu, R. Peng, Q. Wang, Y. Peng, J. Jin, H.-L. Zhang, *Materials Chemistry Frontiers* **2018**, *2*, 1700 – 1706.

[13] a) S. Zhang, X. Zhang, L. Lei, X.-F. Yu, J. Chen, C. Ma, F. Wu, Q. Zhao, B. Xing, *Angew. Chem. Int. Ed.* **2019**, *58*, 467 – 471; *Angew. Chem.* **2019**, *131*, 477 – 481; b) Z. Guo, S. Chen, Z. Wang, Z. Yang, F. Liu, Y. Xu, J. Wang, Y. Yi, H. Zhang, L. Liao, P. K. Chu, X.-F. Yu, *Adv. Mater.* **2017**, *29*, 1703811.

[14] R. Pikl, F. Duschek, C. Fickert, R. Finsterer, W. Kiefer, *Vib. Spectrosc.* **1997**, *14*, 189 – 197.

[15] K. P. S. S. Hembram, H. Jung, B. C. Yeo, S. J. Pai, S. Kim, K.-R. Lee, S. S. Han, *J. Phys. Chem. C* **2015**, *119*, 15041 – 15046.

[16] a) J. D. Corbett, Chemistry, *Structure and Bonding of Zintl phases and Ions*, VCH Publishers, New York, Chapter 3, **1996**; b) H. G. Von Schnering, W. Hoenle, *Chem. Rev.* **1988**, *88*, 243 – 273; c) V. Miluykov, A. Kataev, O. Sinyashin, P. Lönnecke, E. Hey-Hawkins, *Z. Anorg. Allg. Chem.* **2006**, *632*, 1728 – 1732; d) J. M. Sangster, *J. Phase Equilib. Diffus.* **2010**, *31*, 62 – 67.

[17] J. M. Englert, P. Vecera, K. C. Knirsch, R. A. Schäfer, F. Hauke, A. Hirsch, *ACS Nano* **2013**, *7*, 5472 – 5482.

Manuscript received: June 19, 2020
Accepted manuscript online: July 31, 2020
Version of record online: August 31, 2020

